THE BELL SYSTEM TECHNICAL JOURNAL
Vol. 57, No. 7, September 1978
Printed in U.S.A.

Spectral Sharing in Hybrid Spot and Area Coverage Satellite Systems via Channel Coding Techniques

By A. S. ACAMPORA

(Manuscript received December 1, 1977)

Multiple spot-beam switching satellites employing frequency reuse are considered, and a method for incorporating an area coverage beam to provide service to those regions not covered by the footprint of any spot beam is proposed here. The method consists of employing a convolutional code for the area beam transmission to enable sharing of a common spectral band among the spot and area beams on a noninterfering basis and with no sacrifice in the capacity of the spot beams. A maximum-likelihood algorithm for this purpose is derived, and bounds on the bit error rate performance of all beams are found. Results show that excessive performance degradation arising from cochannel interference is limited to a thin annular ring surrounding each spot beam.

I. INTRODUCTION

Multiple spot beam communication satellites offer the potential for greatly increasing the traffic handling capability relative to wide-area coverage systems, since the allocated spectral band can be reused in the various spot beams.[1,2] A high-level block diagram of the satellite transponders for such a system might appear as shown in Fig. 1. Here, the various service regions are interconnected via an on-board switching matrix operating in the time-division mode, and digital modulation techniques consistent with time-division multiple access (TDMA) are employed.

As previously noted,[3] such a system suffers a serious drawback in that a large blackout region, serviceable by none of the spot beams, is created. The situation is depicted in Fig. 2, which shows the radiation footprints of a hypothetical 11-beam private line system serving the large population regions in the United States. Although most of the traffic load for

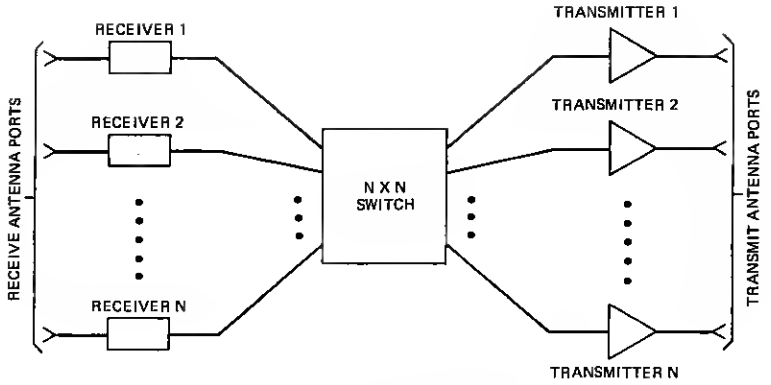

Fig. 1—Satellite transponder.

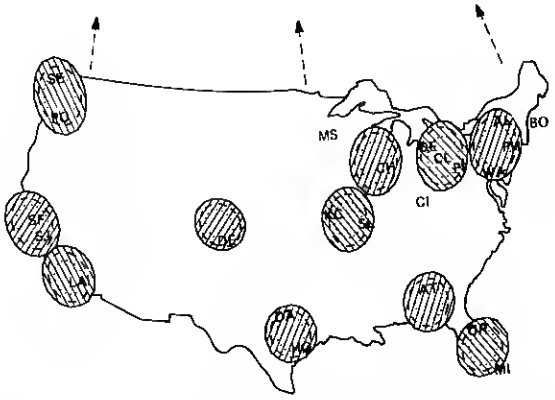

Fig. 2—Footprints of a hypothetical 11-beam system showing −1, −2, and −3 dB contours. Both polarizations are employed.

such an offering would be adequately served by the 11 high-capacity spot beams, it is nonetheless desirable to provide service to the outlying areas.

Among the various techniques proposed in Ref. 3 for coping with this blackout problem, the method of deploying a channel coded area coverage beam, in addition to the various uncoded spot beams, appears most attractive in that the blackout region is reduced to a thin annular ring surrounding each spot beam. This method offers the additional advantage of reducing the required radiated power for the area coverage beam, an important consideration since the gain of the area beam antenna port might be 20 dB lower than that of a spot beam port. In this paper, we review the principles involved in this approach and derive bounds on the resulting bit error rate performance of both the spot and area beams.

In Section II, we discuss the problems associated with sharing a

common spectral band between area coverage and spot coverage satellite beams. Section III is devoted to the derivation of a detection algorithm for such a hybrid system in which convolutional coding is used to alleviate the effects of cochannel interference, and bit error rate bounds are found. In Section IV, these results are applied in a typical communication satellite scenario.

II. PROBLEM DEFINITION

Consider a satellite system consisting of M spot-beam transponders serving M geographically separated, high-traffic demand areas on a noninterfering basis. The allocated spectral band is totally reused in the M spot beams. We wish to deploy an area coverage beam, in addition to the M spot beams, to provide service to the low traffic demand outlying regions serviced by none of the spot beams. The total traffic demand to all outlying regions might be of the same order of magnitude as the demand for one spot beam. Service to the outlying regions must be provided on a noninterfering basis and with no sacrifice to the capacity of the various spot beams. We assume that the spot beams require use of both electromagnetic polarizations to minimize mutual interference among themselves.

Four types of interference are readily identified:

(*i*) *Down-link:* The area coverage radiation is detectable at every spot beam receiving terminal and can thereby interfere with reception of the desired signal at those ground stations.

(*ii*) *Down-link:* The spot beam footprints might typically be useful out to their −3 dB radiation contours. Area-coverage receiving terminals located at the −3 dB through the −20 dB contours of any spot beam thereby suffers interference from that spot beam.

(*iii*) *Up-link:* All up-link transmissions from spot-beam earth terminals are detectable at the antenna port of the area coverage beam and thereby interfere with reception of the area coverage up-link transmission.

(*iv*) *Up-link:* Transmission from an area coverage ground station located between the −3 dB and the −20 dB contour of a spot-beam antenna pattern could interfere with that spot beam's up-link transmission.

Thus, the inclusion of an area beam might make the original spot beams totally unusable. To eliminate these interference problems, one might split the allocated spectral band into two components; one segment would be dedicated to the area coverage transponder and the second segment would be reused among the various spot beams. If this is done, the system designer must choose one of two options:

(*i*) Reduce the throughput of the spot beam transponders by that fraction of the satellite band dedicated to the area coverage beam.

(*ii*) Maintain the original throughput of the spot beam transponders while increasing the effective radiated power on both the up-link and the down-link to overcome the degradation caused by excessive band-limiting.

Option (*i*) results in a sizable decrease in the overall capacity of the satellite. Consider a 10-spot-beam system with each beam occupying the entire spectral band. The normalized throughput of such a system is defined to be 10 units. Suppose that two area coverage beams are added to the system (one using each polarization) and that one-half the band is reserved for the spot beams. Then, under option (*i*), the normalized throughput is reduced to $\frac{1}{2} \times 10 + \frac{1}{2} \times 2 = 6$, and the overall system throughput is reduced by 40 percent. For the same fractional split of the total bandwidth, option (*ii*) could incur a power penalty in excess of 6 dB for a 4ϕ-CPSK (coherent phase shift key) system originally operating at a modest BT (bandwidth-time) product of 1.3. Such a penalty might be acceptable on the up-link, but would typically be unacceptable on the down-link since space platform power is a limited resource.

Thus, to provide service to the outlying area at no sacrifice in either the throughput of the spot beams or in the required spot beam effective isotopic radiated power (e.i.r.p.), one might consider splitting the band, as described above, to eliminate up-link interference. Up-link digits would be regenerated, switched, and reformatted into the appropriate down-link port. A suitable scheme must then be sought to accommodate the down-link.

Channel coding techniques will be investigated as a possibility. The motivation for sucb an approach is twofold. First, and most important, coding can provide for effective immunity against cochannel interference. Second, we note that because of the difference of about 20 dB between the antenna gains of the area and spot-beam coverage antenna ports, a system would require 20 dB more power for the area coverage port than for a spot-beam port to achieve the same bit error rate performance. Through use of coding, we can effect a considerable reduction in the required power for the global beam.

The scenario envisioned, shown in Fig. 3, would employ uncoded transmission for the spot-beam messages and rate $r = \frac{1}{2}$ convolutionally encoded transmission for the area beam port. The throughput of the area beam port would be one-half that of the spot-beam port, implying that the down-link channel symbol rate for all beams are the same. In addition, since on-board regeneration is employed, all down-link channel symbols can be time-aligned. We will consider 4ϕ-CPSK modulation and explore in detail the situation where the in-phase and quadrature rails of both the area and spot coverage beams are modulated separately and where there is no crossrail coupling. Thus, we can consider baseband performance. The algorithms and other results to be presented are

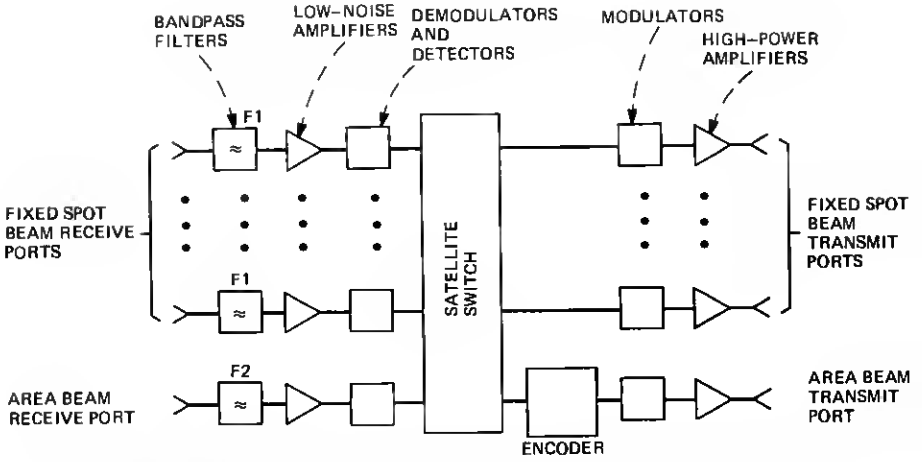

Fig. 3—Regenerative transponder for a hybrid spot-area coverage satellite employing channel coding. The allocated band is split between the spot and area beams on the uplink. The band is totally reused for all the downlinks.

readily generalized to the situation where there is a known, fixed carrier phase shift between the spot and area transmissions.

III. BIT ERROR RATE PERFORMANCE

We now investigate the bit error rate performance of both the uncoded spot beam message and the encoded global beam message in the interference-prone region surrounding one of the spot beams. We need to consider the presence of only one such spot beam since, in the footprint area of that beam, interference from the remaining beams is negligible. At a particular ground station, after coherent demodulation, we observe the following received baseband process:

$$R(t) = \sqrt{E_1} \sum_k b_k h(t - kT) + \sqrt{E_2} \sum_k y_k(\mathbf{a}) h(t - kT) + n(t). \quad (1)$$

In (1) above, b_k is the kth member of the binary data stream $\mathbf{b}$ of the uncoded spot beam message, a represents the binary data stream for the global beam, $y_k(\mathbf{a})$ is the kth channel symbol of the global beam and is dependent upon $\mathbf{a}$ through the structure of the encoder, $h(t)$ is the impulse response of the channel, $n(t)$ is a Gaussian noise process of spectral power density $N_0/2$, and E_1 and E_2 are, respectively, the received pulse energy of the spot and global beam transmissions. We note that the b_k's are independent and equally likely to be ± 1, and that the y_k's can assume the values ± 1 but are not independent. We assume that intersymbol interference is absent.

A set of sufficient statistics[4] for detecting the $\mathbf{a}$ and $\mathbf{b}$ sequences is formed by the synchronous samples of $R(t)$ taken at the opening of the binary eye. One such sample is:

$$r_k = \sqrt{E_1}\, b_k + \sqrt{E_2}\, y_k + n_k. \tag{2}$$

We assume the various n_k's to be independent. From the samples (2), we form the log-likelihood function or path metric[4]

$$\Lambda(\mathbf{a},\mathbf{b}) = 2\sum r_k[\sqrt{E_1}b_k + \sqrt{E_2}y_k(\mathbf{a})] - \sum[\sqrt{E_1}b_k + \sqrt{E_2}y_k(\mathbf{a})]^2 \tag{3}$$

and decide upon those sequences $\hat{\mathbf{a}},\hat{\mathbf{b}}$ for which (3) is maximized.

The maximum-likelihood algorithm to perform optimum detection is similar to the Viterbi algorithm[5] and is illustrated by the state transition diagram of Fig. 4, drawn for a $K = 3$ convolutional code. The state is defined by the contents of the first two stages of the shift register, and knowledge of the starting state and the next bit entering the encoder uniquely determines the next state and the encoded channel symbols generated. We note that, unlike the ordinary Viterbi algorithm for rate $r = \frac{1}{2}$ codes, each transition between states can occur along four paths, rather than one, because two independent uncoded symbols are also

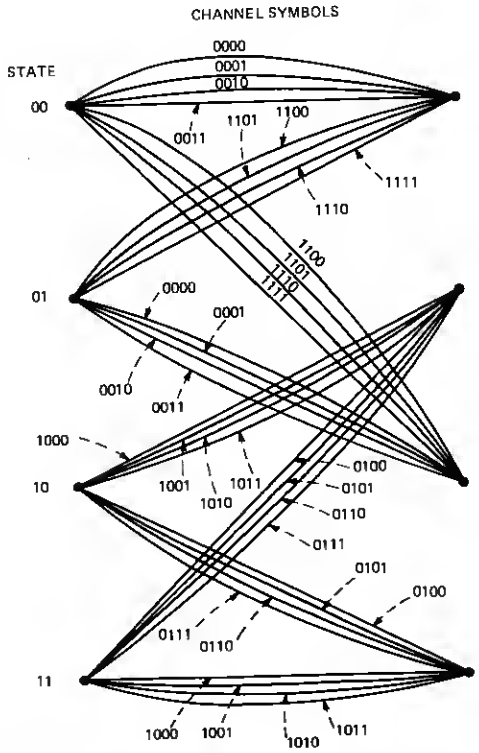

Fig. 4—State diagram for maximum-likelihood detection of interfering coded and uncoded signals. A $K = 3$, $r = \frac{1}{2}$ convolutional code is assumed. For each transition, the first two channel digits correspond to the coded symbols, and the second two correspond to the uncoded symbols.

generated during each epoch. The first two bits appearing along each branch correspond to the encoded channel symbols for that transition, and the second two digits correspond to one of the four possible two-bit sequences for the uncoded transmissions.

To perform maximum-likelihood detection, we note that, at each state, eight possible branches merge, and the partial path metric of one such merging branch must be the largest. The remaining seven paths then cannot be most likely because any succeeding additions to any one of these seven paths are valid additions to that one path exhibiting the greatest partial metric; succeeding additions, then, cannot cause the overall metric of any of these seven paths to exceed that of the path exhibiting greatest partial metric, and the seven paths having the smaller path metrics can be deleted from further consideration.

Thus, at each point in time, the four most likely paths (one leading to each state) and their associated partial metrics are known. During the next clock cycle, we determine the most likely of eight paths leading into each state by performing, for each of two initial states and for each of four branches for each initial state, the operation

$$\Lambda_n = \Lambda_{n-1} + \sum_{k=0}^{1} [2r_{2n-k} - \sqrt{E_1}b_{2n-k} - \sqrt{E_2}\,y_{2n-k}][\sqrt{E_1}b_{2n-k} + \sqrt{E_2}y_{2n-k}] \quad (4)$$

and saving the path and path metric of the largest for subsequent operations. The values of b_{2n-k} and y_{2n-k}, $k = 0,1$ to be substituted into (4) are determined from the state transition diagram, Fig. 4.

To perform true maximum likelihood detection, the most likely path leading into each state must be stored over the entire past. However, it has been shown that after 4 to 5 constraint lengths have elapsed, the oldest bits in all path memories are the same with a very high probability. Thus, we need to save only the most recent 4K through 5K of data for each state and, once in each epoch, the oldest bits in any one of four path memories can be outputted as detected data. We note that, unlike the ordinary Viterbi algorithm for which each path memory consists of a single rail of data, here we need to store three rails of data for each state. One rail contains the most likely source sequence **a** for the area coverage beam, and the second two contain the first and second source bits emitted each epoch for the uncoded spot beam sequence **b**.

The detector will commit an error for the first time at node n if the partial metric of some path which previously diverged from the correct path and remerges at node n is greater than that of the correct path. Some possible error events are shown in Fig. 5. We now calculate the probability of such an event.

Let **A** correspond to the spot and area coverage information sequence along the correct span, and let $\hat{\mathbf{A}}$ be those along the incorrect span. Then, the path metric difference is given by:

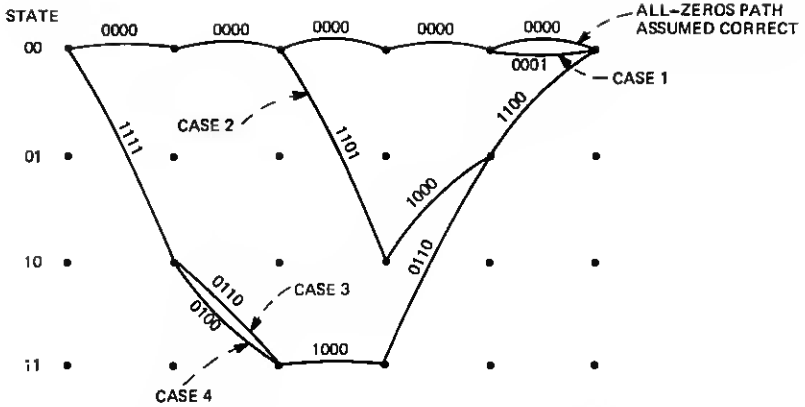

Fig. 5—Select error events for the maximum-likelihood detector.

$$\Lambda(\mathbf{A}) - \Lambda(\hat{\mathbf{A}}) = 2\sum r_k[\sqrt{E_1}(b_k - \hat{b}_k) + \sqrt{E_2}(y_k - \hat{y}_k)] - \sum[(\sqrt{E_1}b_k + \sqrt{E_2}y_k)^2 - (\sqrt{E_1}\hat{b}_k + \sqrt{E_2}\hat{y}_k)^2], \quad (5)$$

where the summation is performed over the unmerged span. Substituting (2) into (5) and recognizing that $b_k^2 = \hat{b}_k^2 = y_k^2 = \hat{y}_k^2 = 1$, we obtain

$$\Lambda(\mathbf{A}) - \Lambda(\hat{\mathbf{A}}) = A + n_{eq}, \quad (6)$$

where

$$A = 4\sum[\sqrt{E_1}\hat{b}_k + \sqrt{E_2}\tilde{y}_k]^2 \quad (7)$$

and

$$n_{eq} = 4\sum n_k[\sqrt{E_1}\hat{b}_k + \sqrt{E_2}\tilde{y}_k]. \quad (8)$$

In (7) and (8), we have used the nomenclature

$$\hat{b}_k = \begin{cases} b_k & \text{if } \hat{b}_k = b_k \\ 0, & \text{otherwise.} \end{cases} \quad (9)$$

$$\tilde{y}_k = \begin{cases} y_k & \text{if } \hat{y}_k = y_k \\ 0, & \text{otherwise.} \end{cases} \quad (10)$$

The first event error probability P is equal to the probability that $\Lambda(\mathbf{A}) - \Lambda(\hat{\mathbf{A}}) < 0$. From (6) through (8), we conclude that

$$P = Q\left\{\sqrt{\frac{2\sum(\sqrt{E_1}\hat{b}_k + \sqrt{E_2}\tilde{y}_k)^2}{N_0}}\right\}, \quad (11)$$

where Q is the complimentary error function. From this result, we now derive upper bounds on the bit error rate performance of the coded and uncoded transmission. We do the uncoded first.

Let the unmerged span be L channel digits long. We see from (11) that the first event error probability is dependent upon the correct sequence

along the unmerged span. For each possible error path of length L, we will determine the number of uncoded bit errors experienced along that path, and average (11) over all possible correct sequences. An upper bound on the average bit error rate for the uncoded transmission is then given by the summation over all possible incorrect paths, of the product of the number of bit errors experienced along a particular path and the average probability that the particular path has a metric exceeding that of the correct path.

Let the coded channel bits be different along the correct and incorrect paths in D symbols. Let the number of channel symbols for which an error occurs for both the coded and uncoded bits be denoted by r, and let the number of channel symbols for which an error occurs for the uncoded, but not for the coded, be denoted by s. Since the uncoded transmissions are equally likely to be ± 1, then along any L,D,r,s path, the coded and uncoded symbols may add or subtract, depending on the particular correct path. In $1/2^r$ of the paths, the correct symbols of the coded and uncoded transmissions will algebraically subtract over all r symbols. Similarly, in $\binom{r}{j}/2^r$ of the paths, there will be a subtraction in $(r-j)$ symbols and an addition in j symbols. In s symbols, $\tilde{b}_k^2 = 1$ and $y_k = 0$, while in $(D-r)$ symbols, $\tilde{b}_k = 0$ and $\tilde{y}_k^2 = 1$. There are $r+s$ errors committed in the uncoded transmission. Thus, averaging over all possible correct paths of the same L,D,r,s, we obtain the result that the average probability of error for each path of the same L and D for the uncoded transmission is given by

$$P_b = \frac{1}{2} \sum_{s=0}^{L-D} \sum_{r=0}^{D} \binom{L-D}{s} \binom{D}{r} \frac{r+s}{2^r} \sum_{j=0}^{r} \binom{r}{j} Q(r,s,j,D), \tag{12}$$

where

$$Q(r,s,j,D) \triangleq Q \left\{ \sqrt{\frac{2}{N_0}} [(r-j)(\sqrt{E_1} - \sqrt{E_2})^2 + j(\sqrt{E_1} + \sqrt{E_2})^2 + (D-r)E_2 + sE_1 \right\}. \tag{13}$$

The factor of $1/2$ appearing in front of (12) arises from the fact that two uncoded bits are transmitted per epoch.

Using the inequality that for $x \geq 0, y \geq 0$,

$$Q\{\sqrt{x+y}\} \leq Q\{\sqrt{x}\} e^{-y/2}, \tag{14}$$

we can overbound and simplify (12) and (13) to the following:

$$P_b \leq Q \left\{ \sqrt{\frac{2DE_2}{N_0}} \right\} e^{-E_1/N_0} [DXe^{E_1/N_0} + L(1+X) - D] \times [(1+X)^{D-1}(1+e^{-E_1/N_0})^{L-D-1}], \tag{15}$$

where

$$X \triangleq \frac{1 + e^{-4\sqrt{E_1E_2}/N_o}}{2} e^{-(E_1-2\sqrt{E_1E_2})/N_o}. \tag{16}$$

Finally, for a particular convolutional code, we use the code generating function matrix method of Viterbi[5] to identify all L,D paths for that code, and sum the contribution (15) for each such path over all possible paths. To this result must be added the contribution of the trivial case for which no coded errors occur (see Fig. 5, case 1). The contribution of these paths is simply

$$P_b = Q\left\{\sqrt{\frac{2E_1}{N_o}}\right\} + Q\left\{\sqrt{\frac{4E_1}{N_o}}\right\}. \tag{17}$$

The results of this exercise have been applied to the optimum $K = 7$, $r = \frac{1}{2}$ code,[6] and appear in Fig. 6. Plotted there is the uncoded bit error rate bound vs the required energy per information bit-to-noise ratio, e_b/N_o, for various ratios of interference to signal (E_2/E_1). Also plotted is the ideal, interference-free performance. We see here that as E_2/E_1 decreases below 2.5 dB, performance starts to improve. The utility of the maximum likelihood sequence estimation (MLSE) to detect uncoded transmission in the presence of coded area coverage interference is il-

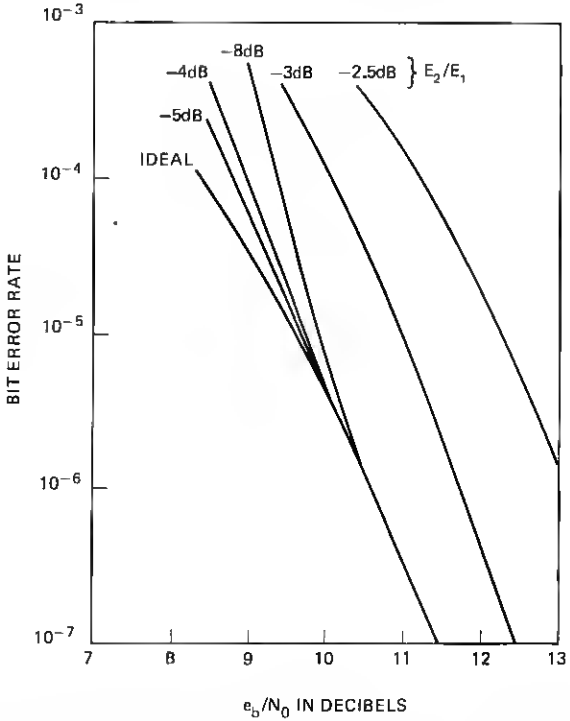

Fig. 6—Bound on uncoded bit error rate performance of maximum-likelihood detector vs e_b/N_o for select values of interference.

lustrated by the following example. Suppose $E_2/E_1 = -3$ dB. Then, if simple bit-by-bit detection is performed, an asymptotic degradation of about 10 dB from ideal would be expected. However, through use of the MLSE, the asymptotic degradation is about 1 dB.

We also see from these curves that, as E_2/E_1 decreases below about -8 dB, there is an apparent degradation in performance. This virtual result is caused by the bounding technique used, and is not experienced in practice. To see how this arises, we note that, as E_2/N_0 becomes small, all paths through the decoding trellis exhibiting a fixed number N of uncoded bit errors become equally likely. The contribution of each such path to the bit error rate bound is, however, summed, indicating a much higher bit error rate than would actually be encountered since only one such incorrect path could actually be selected at any node. For sufficiently small E_2/N_o, in fact, the bound no longer converges. To evaluate performance of the MLSE in the regime where the bound converges poorly, extensive simulation studies were performed and are shown in Fig. 7. These studies show that there is in fact a degradation in performance as E_2/E_1 decreases below -4 dB, but that the worst-case degradation of about 1 dB from ideal occurs for $E_2/E_1 = -10$ dB. As the in-

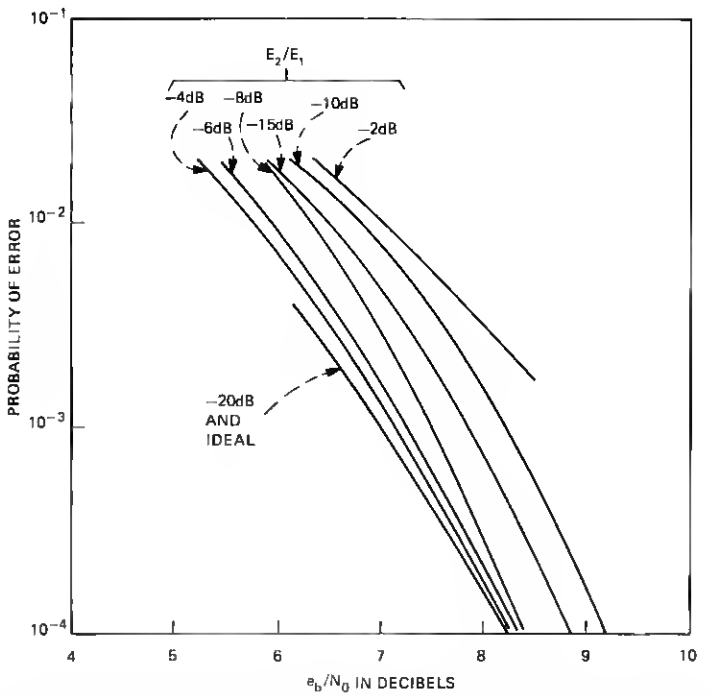

Fig. 7—Uncoded bit error rate performance of maximum-likelihood detector vs e_b/N_o obtained via simulation for select values of interference.

terference becomes smaller, performance begins to approach the ideal, interference-free case as intuitively expected.

We now study the performance of the encoded area beam. Again, let the unmerged span be L channel digits long and let the coded digits be different along the correct and incorrect paths in D channel symbols and N information symbols. Then, averaging overall possible combinations of the uncoded symbols, the average number of area beam bit errors incurred along any L,D,N path is given by:

$$P_b = N \sum_{s=0}^{L-D} \sum_{r=0}^{D} \binom{L-D}{s} \binom{D}{r} \frac{1}{2^r} \sum_{j=0}^{r} \binom{r}{j} Q(r,s,j,D), \tag{18}$$

where $Q(r,s,j,D)$ is given by (13). Invoking inequality (14), we obtain the bound:

$$P_b \leq N e^{-DE_2/N_0} (1 + e^{-e_1/N_0})^{L-D} (1 + X)^D, \tag{19}$$

where X is given by (16). Once again, we use the generating function matrix approach to determine the contribution of each incorrect path.

Results for the optimum $K = 7$ code appear in Fig. 8. Shown there is the bit error rate performance of the encoded area beam message vs e_b/N_o for select values of E_1/E_2, the interference-to-signal ratio. We see that, when E_1 becomes much greater than E_2, performance approaches the ideal, interference-free case since, under these conditions, the MLSE algorithm exploits the large difference between the signal and interference strengths to correctly decode the small signal. For $E_2 > E_1$, the bounding technique again suffers from poor convergence properties, and the results are meaningless. Again, extensive simulation studies were performed and are shown in Fig. 9. We see that, as expected, the ideal interference-free case is approached as E_1/E_2 becomes small.

For all values of E_1/E_2, the MLSE algorithm provides the best attainable performance. However, when E_1/E_2 becomes sufficiently small, the improvement possible via MLSE becomes negligible as shown by the plots of Fig. 10. These data were obtained experimentally and show the bit error rate performance of the ordinary Viterbi algorithm in the presence of a single bit-synchronous cochannel interferer. The ordinary Viterbi algorithm operates as though no interference was present and, unlike the MLSE algorithm, would be useless for $E_1 > E_2$. However, for $E_1 \ll E_2$, performance of the two are about the same, and the slight improvement possible via MLSE is not warranted in view of the additional complexity incurred.

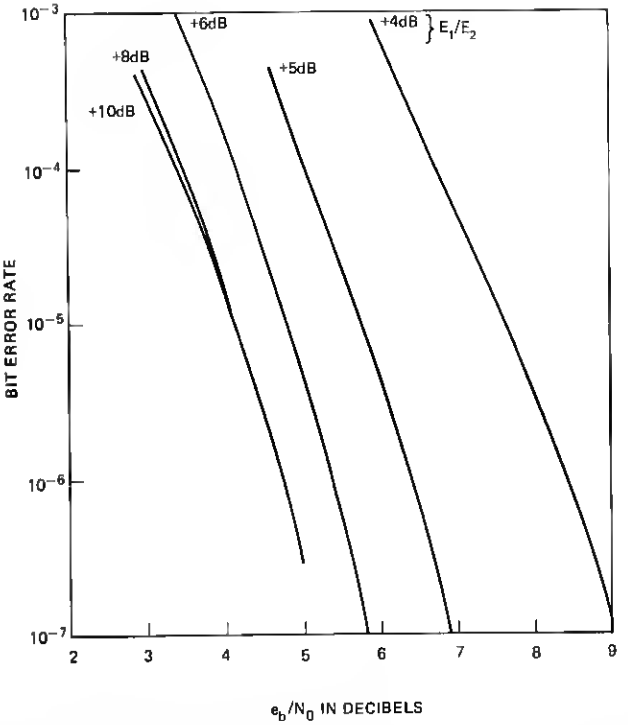

Fig. 8—Bound on coded bit error rate performance of maximum-likelihood detector vs e_b/N_0 for select values of interference.

IV. APPLICATION

We now apply the results of the preceding section to the problem of reducing mutual interference between spot and area coverage beams sharing a common spectral band. Let the spot-beam radiation pattern be Gaussian-shaped and usable to its −3 dB contour. In the absence of cochannel interference, the e.i.r.p. of the coded global beam would be 8 dB lower than that of the spot beam at its −3 dB contour for the same system outage and bit error rate (BER) performance. This 8-dB factor can be broken down into a 3-dB component, since the information rate of the global beam is half that of the spot beam, plus a 5-dB component representing the coding gain of a $K = 7$, $r = \frac{1}{2}$ convolutional code. Suppose we set E_2/E_1 at the 3-dB contour of the spot beam at −8 dB. Then, throughout the spot-beam coverage area, $-11 \text{ dB} \leq E_2/E_1 \leq -8 \text{ dB}$. From Fig. 6, we see that, over this range, the BER performance of the uncoded spot-beam message is degraded by at most 1 dB if MLSE is employed. By contrast, if bit-by-bit detection of the spot-beam message were employed, the degradation would be between 2.9 dB and 4.4 dB.

Let the e.i.r.p. of both the spot and area coverage beams rise by 1 dB.

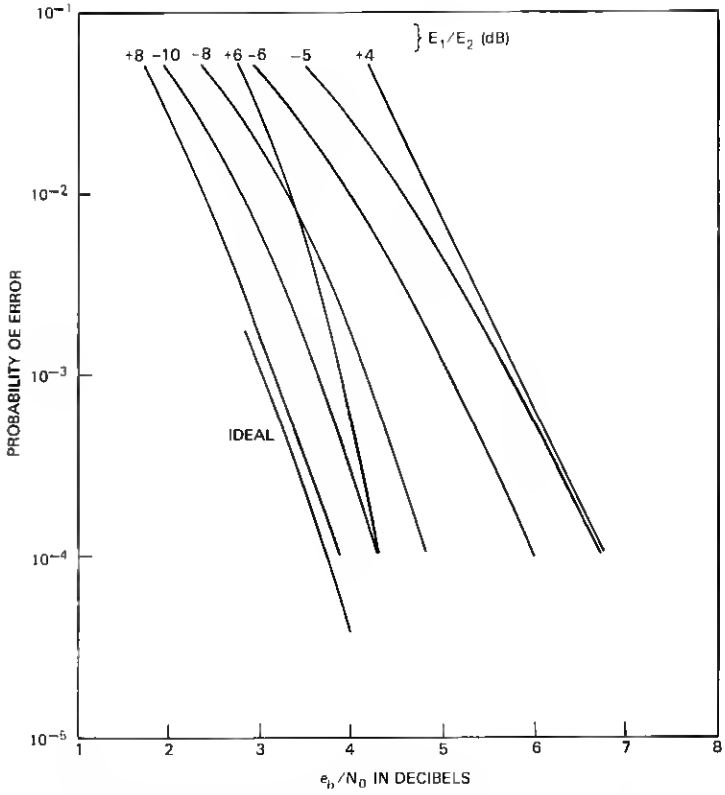

Fig. 9—Coded bit error rate performance of maximum likelihood detector vs e_b/N_o obtained via simulation for select values of interference.

Then, throughout the spot-beam coverage region, the BER performance is at least as good as that obtained in the absence of interference with 1 dB less power. From Fig. 8, we see that, beyond the −3 dB contour of the spot beam, we can communicate via the area coverage beam in conjunction with MLSE with at most 1-dB degradation from the ideal interference-free situation provided $E_1/E_2 > 5.5$ dB. Finally, from Fig. 10, we see that we can use the area beam with the ordinary Viterbi algorithm provided $E_1/E_2 < -12$ dB. From these observations, we can construct the plot of Fig. 11, which shows the one-dimensional radiation patterns of a spot beam and the area beam and the usable regions for the spot and area coverage beams in the vicinity surrounding a spot beam. Implicit in this illustration is the fact that the e.i.r.p. of both the spot and area beams is increased by 1 dB to provide the same grade of service as possible with 1 dB less power in the absence of cochannel interference. We see that communication via the spot beam, in conjunction with MLSE, is employed out to the −3 dB contour of the spot beam. From $\theta = \theta_{3\text{dB}}$ out to $\theta = 1.4\theta_{3\text{dB}}$, we can communicate via the area beam, even though

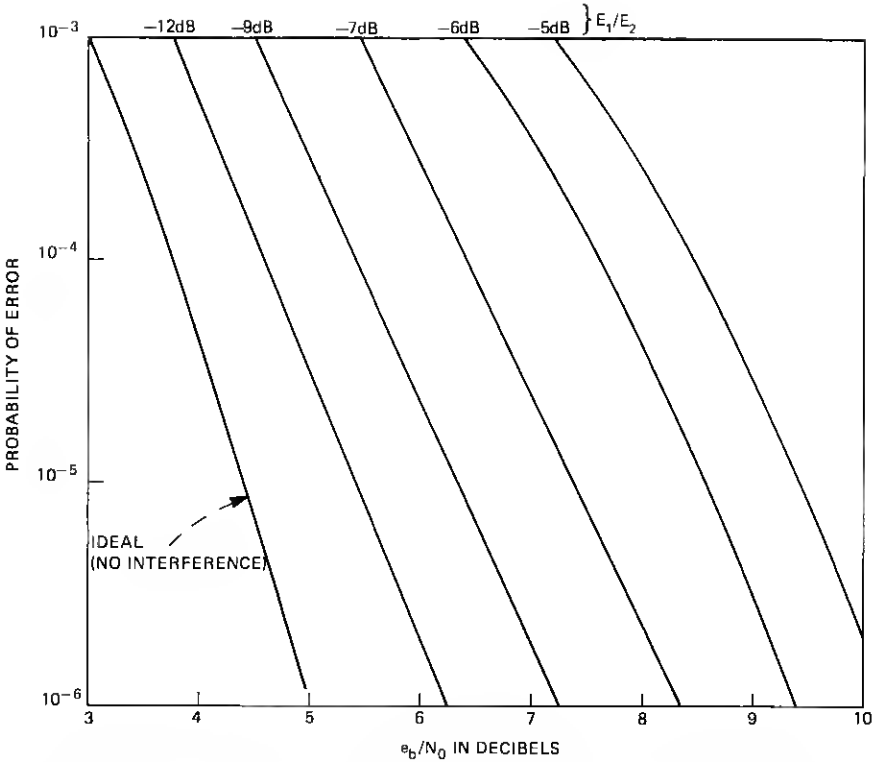

Fig. 10—Measured bit error rate performance of a $K = 7$, $r = \frac{1}{2}$ convolutional code vs e_b/N_o for select values of interference. The interference is bit-synchronous with the encoded channel bits, and the ordinary Viterbi algorithm with soft (3-bit) quantization is employed.

the interference is stronger than the desired signal. Between $\theta = 1.4\theta_{3dB}$ and $\theta = 2.75\theta_{3dB}$, the performance degradation of the area beam exceeds the allotted 1 dB, and the desired grade of service cannot be provided. This region, then, is blacked out. Finally, for $\theta > 2.75\theta_{3dB}$, communication via the global beam is again possible.

Thus, through utilization of an area coverage beam in conjunction with channel coding and MLSE, the blackout region of a multiple spot-beam communication satellite is reduced from the entire region not serviced by any spot beam to a thin annular ring surrounding each spot beam. There is no sacrifice in the capacity of the spot beams, and the power penalty is 1 dB for all beams.

Let us now consider a specific example. We assume the existence of 10 spot beams, half of which employ one polarization and half the orthogonal polarization. In the absence of interference, each spot beam transponder uses a 3-watt final power amplifier, and the difference between the spot and area beam antenna gains is 20 dB. Suppose we deploy

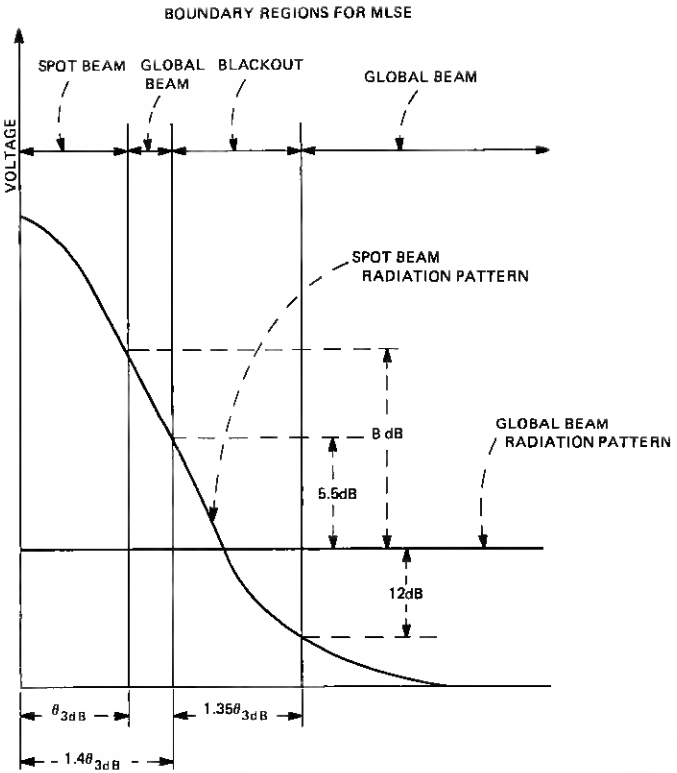

Fig. 11—One-dimensional plot showing the usable regions attainable via MSLE for a hybrid spot-area beam satellite system employing a $K = 7$, $r = 1/2$ code for the area beam transmission. The spot beam antenna pattern is Gaussian shaped.

a single-area beam transponder employing one of the two polarizations; the capacity of this beam is one-half that of a spot beam, and a $K = 7$, $r = \frac{1}{2}$ code is employed. In the absence of interference, the RF power required of the area beam would be $20 - 8 = 12$ dB higher than any spot beam. The total required RF power for the hybrid system outlined above is then

$$P = 1.25 \times [3 \times 10 + 47.5] = 97 \text{ watts.} \tag{20}$$

By contrast, if we employ the band-splitting technique described in Section II, we would need 6 dB more power for each spot beam, and the power required for the area beam would be 17 dB higher than that required for the spot beam in the absence of interference, since coding is not employed. The total power, then, would be

$$P = 4 \times 3 \times 10 + 50.1 \times 3 = 270 \text{ watts.} \tag{21}$$

Considering a 30-percent efficiency for the final TWT, the total dc power

required via coding is 323 watts, while that needed for the alternative band-splitting approach is 900 watts.

Since, through use of coding, the dc power required for an area beam is only 158 watts, we might consider deploying a second area beam using the orthogonal polarization. Then, not only do we double the capacity into the outlying region, but we also eliminate the blackout region, since each spot beam is used in only one polarization. Area coverage communication to the blackout region of one polarization can thereby be provided in the second polarization. The dc power required for this approach is 442 watts.

V. MAXIMUM-LIKELIHOOD ALGORITHM WITH FIXED PHASE SHIFT

In Section III, we derived a maximum-likelihood algorithm which allows joint area and spot-beam coverage sharing a common spectral band whenever there is no carrier phase shift difference between the area and spot beam transmissions. We now derive the proper algorithm for use when there is a fixed phase shift difference, θ. During the kth clock cycle, the spot beam source emits two bits, $b_{1,k}$ and $b_{2,k}$, and the area beam source emits a single bit a_k and two encoded channel bits $y_{1,k}(\mathbf{a})$ and $y_{2,k}(\mathbf{a})$. The data $b_{1,k}$ and $b_{2,k}$ are modulated onto a carrier via 4ϕ-PSK, as are $y_{1,k}$ and $y_{2,k}$. Thus, we transmit:

$$R(t) = \sqrt{E_1}b_{1,k}\cos(\omega t + \theta) + \sqrt{E_1}b_{2,k}\sin(\omega t + \theta) + \sqrt{E_2}y_{1,k}\cos\omega t + \sqrt{E_2}y_{2,k}\sin\omega t. \quad (22)$$

The receiver locks onto the phase of the encoded area beam and, during the kth clock cycle, the receiver observes, after coherent demodulation, the two test statistics:

$$r_{1,k} = \sqrt{E_2}y_{1,k} + \sqrt{E_1}b_{1,k}\cos\theta + \sqrt{E_1}b_{2,k}\sin\theta + n_{1,k} \quad (23)$$

$$r_{2,k} = \sqrt{E_2}y_{2,k} - \sqrt{E_1}b_{1,k}\sin\theta + \sqrt{E_1}b_{2,k}\cos\theta + n_{2,k}. \quad (24)$$

The path metric now takes the form:

$$\Lambda(\mathbf{a},\mathbf{b}) = \sum_k [r_{1,k}(\sqrt{E_2}y_{1,k} + \sqrt{E_1}b_{1,k}\cos\theta + \sqrt{E_1}b_{2,k}\sin\theta) + r_{2,k}(\sqrt{E_2}y_{2,k} - \sqrt{E_1}b_{1,k}\sin\theta + \sqrt{E_1}b_{2,k}\cos\theta)] - \sqrt{E_1E_2}[y_{1,k}(b_{1,k}\cos\theta + b_{2,k}\sin\theta) - y_{2,k}(b_{1,k}\sin\theta - b_{2,k}\cos\theta)]. \quad (25)$$

As before, we define the state of the encoder by the contents of the first $K-1$ stages of its shift register, and each state can be accessed via eight paths. Along each path, we compute the partial metric:

$$\Lambda_k(\mathbf{a},\mathbf{b}) = \Lambda_{k-1}(\mathbf{a},\mathbf{b}) + \sqrt{E_2}r_{1,k}y_{1,k} + \sqrt{E_2}r_{2,k}y_{2,k} + \sqrt{E_1}(r_{1,k} - \sqrt{E_2}\,y_{1,k})(b_{1,k}\cos\theta + b_{2,k}\sin\theta) - \sqrt{E_1}(r_{2,k} - \sqrt{E_2}\,y_{2,k})(b_{1,k}\sin\theta - b_{2,k}\cos\theta), \quad (26)$$

and save the path and metric of the larger. Thus, with a fixed known phase shift, maximum-likelihood decoding is also possible.

VI. CONCLUSIONS

In multiple spot-beam communication satellite systems, it is often desirable to provide service to remote areas not covered by any spot beam. This additional service should neither diminish the capacity of the spot beams nor cause a severe downlink power penalty. We considered deployment of an area beam transponder, in addition to the fixed spot beams, and saw that satisfaction of the above requirements implies considerable downlink cochannel interference at all ground stations located in the vicinity of any spot beam. The use of binary convolutional codes for the area beam transmission was shown to greatly curtail the performance degradation resulting from this cochannel interference and also reduce the prime power requirements of the area beam transponder.

A maximum-likelihood algorithm was derived to optimally detect either the uncoded spot beam transmission or the coded area beam transmission, and performance of this algorithm was evaluated. Use of this algorithm was shown to provide for reliable spot-beam communication in the presence of cochannel interference. It is also possible to reliably communicate via the global beam in the presence of a much stronger spot-beam interference. These results were then applied to a scenario in which interference was reduced on the uplink via the simple technique of band-splitting between the area and spot beams. Such a technique is unsuitable for the downlink because of the power penalty incurred. On board, the uplink bits are regenerated and switched into the appropriate downlink beam, and a $K = 7$, $r = \frac{1}{2}$ code is employed for the downlink area beam. Results show that the degradation from cochannel interference is contained to be less than 1 dB over the entire service area except for a thin annular ring surrounding each spot beam. Traffic originating within or destined for these blackout rings might be backhauled to the nearest serviceable region, or else a second area beam, employing the dual polarization, might be deployed such that, for any given spot beam, the blackout region is contained to only one polarization. Since the spot beams use both polarizations to minimize interference among themselves, the MLSE algorithm must still be used at all spot-beam ground stations to provide spot-beam service with minimal performance degradation.

The satellite prime power demands to satisfy RF radiated power requirements were evaluated and shown to be within the capability of the Thor-Delta class. Thus, the use of spot and area coverage beams, sharing a common spectral band, in conjunction with channel coding techniques, appears to be an acceptable method for providing universal service via high-capacity digital switching satellites of the future.

VII. ACKNOWLEDGMENTS

The author wishes to thank his colleagues, D. O. Reudink and Y. S. Yeh, for their stimulating discussions and contributions, and also Mrs. Phyllis Arnold who wrote the programs for the simulation studies.

REFERENCES

1. L. C. Tillotson, "A Model of a Domestic Satellite Communication System." B.S.T.J., *47*, No. 10 (December 1968), pp. 2111–2137.
2. R. Cooperman and W. G. Schmidt, "Satellite Switched SDMA and TDMA Systems for Wideband Multi-Beam Satellite," ICC Conference Record, 1973.
3. A. S. Acampora, D. O. Reudink, and Y. S. Yeh, "Spectral Re-Use in 12 GHz Satellite Communication Systems," ICC Conference Record, 1977.
4. H. L. Van Trees, *Detection, Estimation, and Modulation Theory*, Part I, New York; Wiley, 1968.
5. A. J. Viterbi, "Convolutional Codes and Their Performance in Communication Systems," IEEE Trans. Comm. Tech., *COM-19* (October 1971), pp. 751–772.
6. K. S. Gilhousen, "Coding Systems Study for High Data Rate Telemetry Links," Linkabit Corporation, San Diego, California, January 1971.